Обзор ArXiv/astro-ph, 13-18 декабря 2020

От Сильченко О.К.

ArXiv: 2012.06258

Dwarf Galaxies and the Black–Hole Scaling Relations

Andrew King[1,2,3] & Rebecca Nealon[1,4,5]

[1] *Department of Physics & Astronomy, University of Leicester, Leicester LE1 7RH UK*
[2] *Astronomical Institute Anton Pannekoek, University of Amsterdam, Science Park 904, NL-1098 XH Amsterdam, The Netherlands*
[3] *Leiden Observatory, Leiden University, Niels Bohrweg 2, NL-2333 CA Leiden, Netherlands*
[4] *Centre for Exoplanets and Habitability, University of Warwick, Coventry CV4 7AL, UK*
[5] *Department of Physics, University of Warwick, Coventry CV4 7AL, UK*

14 December 2020

ABSTRACT

The sample of dwarf galaxies with measured central black hole masses M and velocity dispersions σ has recently doubled, and gives a close fit to the extrapolation of the $M \propto \sigma$ relation for more massive galaxies. We argue that this is difficult to reconcile with suggestions that the scaling relations between galaxies and their central black holes are simply a statistical consequence of assembly through repeated mergers. This predicts black hole masses significantly larger than those observed in dwarf galaxies unless the initial distribution of uncorrelated seed black hole and stellar masses is confined to much smaller masses than earlier assumed. It also predicts a noticeable flattening of the $M \propto \sigma$ relation for dwarfs, to $M \propto \sigma^2$ compared with the observed $M \propto \sigma^4$. In contrast black hole feedback predicts that black hole masses tend towards a universal $M \propto \sigma^4$ relation in all galaxies, and correctly gives the properties of powerful outflows recently observed in dwarf galaxies. These considerations emphasize once again that the fundamental physical black-hole — galaxy scaling relation is between M and σ. The relation of M to the bulge mass M_b is acausal, and depends on the quite independent connection between M_b and σ set by stellar feedback.

Две конкурирующие модели:

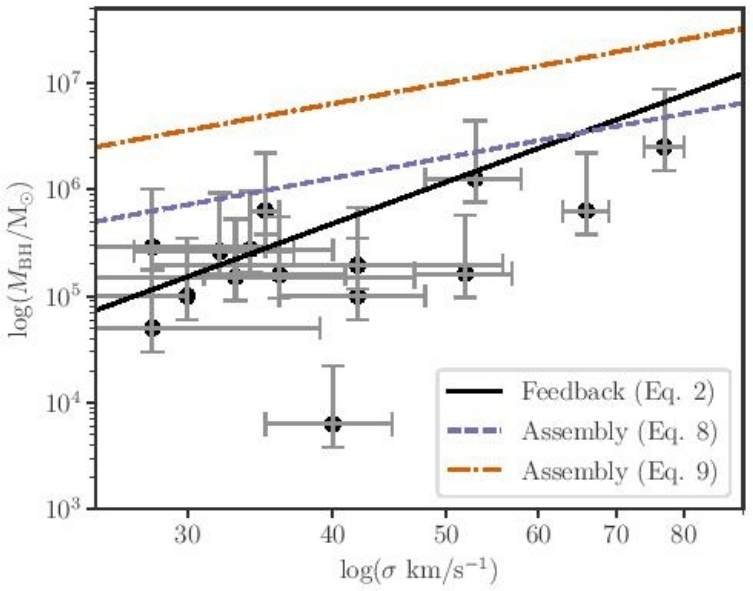

Figure 1. M-σ relation using the data from Baldassare et al. 2020 and the references quoted therein. The $M \propto \sigma^2$ relations (8, 9) predicted by the assembly picture are the orange (dashed) and blue (dash–dot) lines, while the black (solid) curve is the original $M \propto \sigma^4$ relation (2) predicted by feedback.

- BH feedback (2)→ верхняя огибающая $M(BH)=3x10^8(\sigma/200)^4$
- Merging → M(BH)~M(bul) → Для карликов (σ < 100 km/s)

$M(BH)=2x10^6\,(\sigma/50)^2$ (8)

С новыми данными Baldassare+(2020)

Квадратичная зависимость!

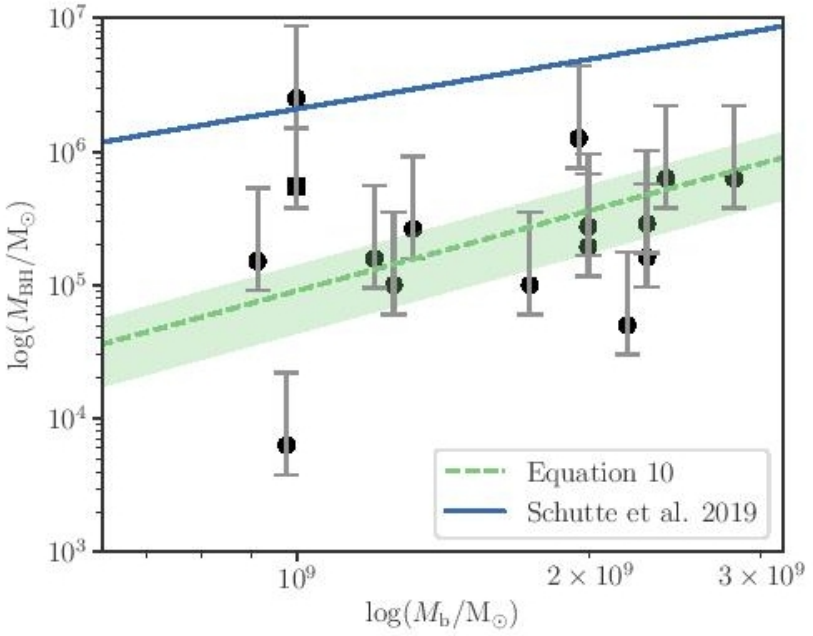

Figure 2. The quadratic $M - M_b$ relation (10, with best–fit value $R_b = 2.3 \pm 1.1$ kpc) for low–mass galaxies plotted against the data from Table 1 of Baldassare et al (2020) and references therein, together with the point from Davis et al., (2020) (as a square). The best–fit linear $M - M_b$ relation found by Schutte, Reines & Greene (2019) for the full SMBH sample for all galaxies is plotted for comparison. This used photometric modeling and colour–dependent mass–to–light ratios to determine M_b.

Объясняет то, что не смогли объяснить Schutte(2019):

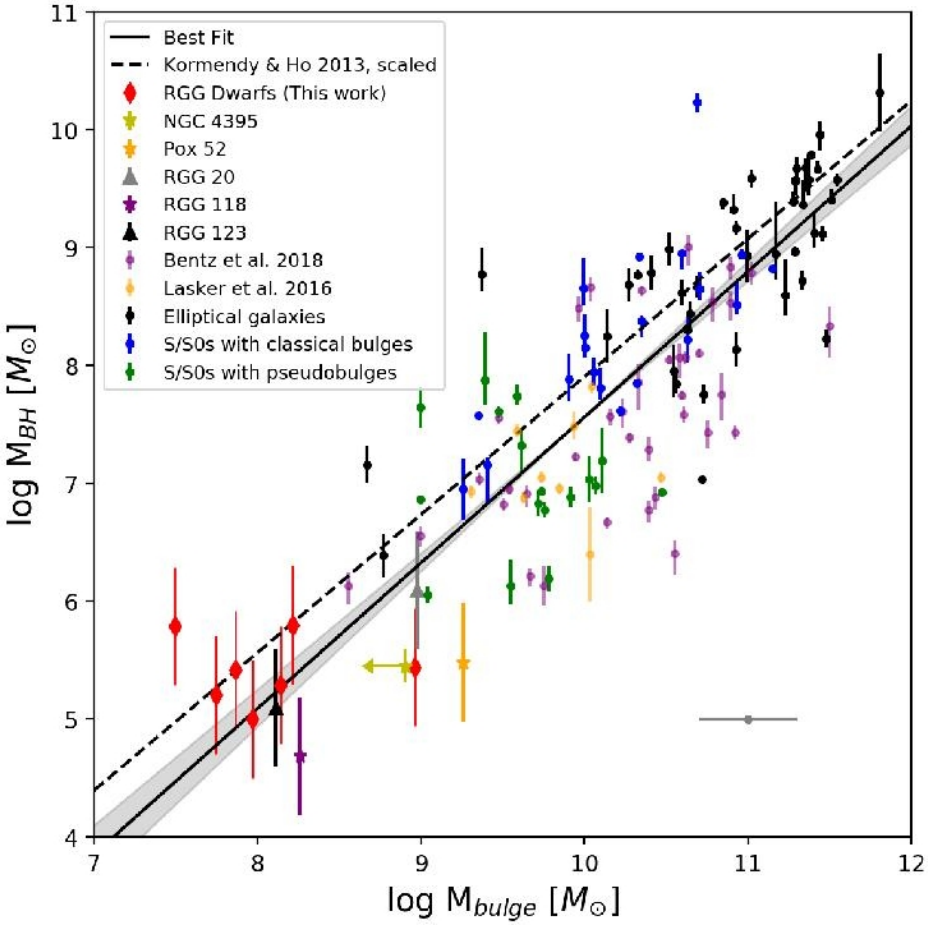

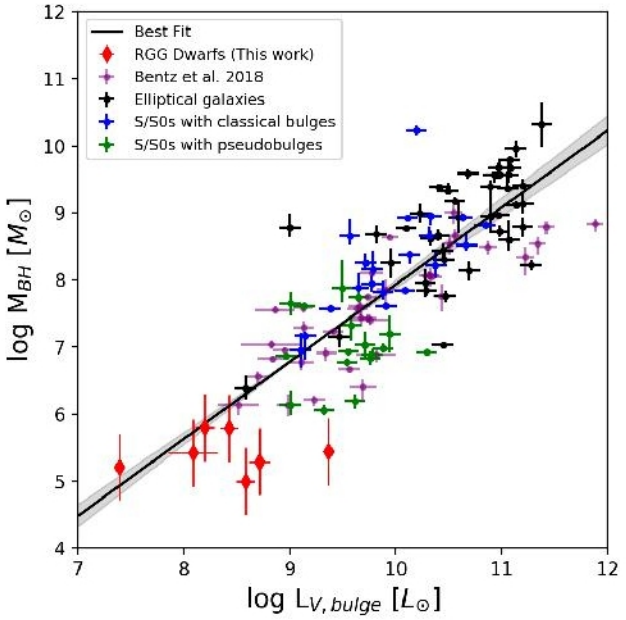

Figure 5. Black hole mass versus bulge V band luminosity. Our sample of 7 broad-line AGN and composite dwarf galaxies from Reines et al. (2013) with new *HST* observations are shown as red diamonds. Dynamical BH mass measurements from Kormendy & Ho (2013) are shown as black (elliptical galaxies), blue (S/S0 galaxies with classical bulges) and green (S/S0 galaxies with pseudobulges) points. Galaxies with reverberation mapped AGNs from Bentz & Manne-Nicholas (2018) are shown as purple points. The best fit linear regression to our sample of dwarf galaxy systems and the entire comparison sample is shown as the solid black line, with the gray shading corresponding to 1 σ uncertainties in the fit parameters.

ArXiv: 2012.08138

The coherent motion of Cen A dwarf satellite galaxies remains a challenge for ΛCDM cosmology⋆

Oliver Müller[1], Marcel S. Pawlowski[2], Federico Lelli[3], Katja Fahrion[4], Marina Rejkuba[4], Michael Hilker[4], Jamie Kanehisa[2,5], Noam Libeskind[2], and Helmut Jerjen[6]

[1] Observatoire Astronomique de Strasbourg (ObAS), Universite de Strasbourg - CNRS, UMR 7550 Strasbourg, France
e-mail: oliver.muller@astro.unistra.fr
[2] Leibniz-Institut fur Astrophysik Potsdam (AIP), An der Sternwarte 16, D-14482 Potsdam, Germany
[3] School of Physics and Astronomy, Cardiff University, Queens Buildings, The Parade, Cardiff,CF24 3AA, UK
[4] European Southern Observatory, Karl-Schwarzschild Strasse 2, 85748, Garching, Germany
[5] Department of Physics, University of Surrey, Guildford GU2 7XH, UK
[6] Research School of Astronomy and Astrophysics, Australian National University, Canberra, ACT 2611, Australia

ABSTRACT

The plane-of-satellites problem is one of the most severe small-scale challenges for the standard ΛCDM cosmological model: several dwarf galaxies around the Milky Way and Andromeda co-orbit in thin, planar structures. A similar case has been identified around the nearby elliptical galaxy Centaurus A (Cen A). In this Letter, we study the satellite system of Cen A adding twelve new galaxies with line-of-sight velocities from VLT/MUSE observations. We find 21 out of 28 dwarf galaxies with measured velocities share a coherent motion. Similarly flattened and coherently moving structures are found only in 0.2% of Cen A analogs in the Illustris-TNG100 cosmological simulation, independently of whether we use its dark-matter-only or hydrodynamical run. These analogs are not co-orbiting, and arise only by chance projection, thus they are short-lived structures in such simulations. Our findings indicate that the observed co-rotating planes of satellites are a persistent challenge for ΛCDM, which is largely independent from baryon physics.

28 спутников CenA

Table 1. Members of Cen A used in this study. For KKs 59 we adopted the same distance as Cen A because there is no accurate TRGB distance available. (a): galaxy name, (b): alternative PGC name, (c): right ascension in epoch J2000, (d): declination in epoch J2000, (e) galaxy distance, and reference for the distance measurement, (f): galaxy heliocentric velocity and reference for the velocity measurement, (g): the technique of the velocity measurement, and (e): de Vaucouleurs morphological type according to the Local Volume catalog (Karachentsev et al. 2004, 2013).

Galaxy Name	Alternative name	α_{2000} (degrees)	δ_{2000} (degrees)	D (Mpc)	v_h (km s^{-1})	Source	Type
(a)	(b)	(c)	(d)	(e)	(f)	(g)	(e)
ESO 269-037	PGC045916	195.8875	−46.5842	3.15±0.09 (1)	744±2 (2)	HI	dIrr
NGC 4945	PGC045279	196.3583	−49.4711	3.72±0.03 (3)	563±3 (4)	HI	Scd
ESO 269-058	PGC045717	197.6333	−46.9908	3.75±0.02 (1)	400±18 (5)	HI	dIrr
KK 189	PGC166158	198.1883	−41.8320	4.21±0.17 (6)	753±4 (7)	stars	dSph
ESO 269-066	PGC045916	198.2875	−44.8900	3.75±0.03 (1)	784±31 (8)	stars	dSph
NGC 5011C	PGC045917	198.2958	−43.2656	3.73±0.03 (1)	647±96 (9)	stars	Tr
KKs 54	PGC2815821	200.3829	−31.8864	3.75±0.10 (10)	621±11 (7)	stars	Tr
KK 196	PGC046663	200.4458	−45.0633	3.96±0.11 (1)	741±15 (11)	stars	dIrr
NGC 5102	PGC046674	200.4875	−36.6297	3.74±0.39 (3)	464±18 (12)	HI	Sa
KK 197	PGC046680	200.5086	−42.5359	3.84±0.04 (1)	643±3 (7)	stars	dSph
KKs 55	PGC2815822	200.5500	−42.7311	3.85±0.07(1)	530±14 (7)	stars	Sph
dw1322-39		200.6336	−39.9060	2.95±0.05 (10)	656±10 (7)	stars	dIrr
dw1323-40b		200.9809	−40.8361	3.91±0.61 (10)	497±12 (7)	stars	dSph
dw1323-40a		201.2233	−40.7612	3.73±0.15 (10)	450±14 (7)	stars	dSph
Cen A	PGC046957	*201.3667*	*−43.0167*	*3.68±0.05 (1)*	*556±10 (4)*	HI	$S0^0$
KK 203	PGC166167	201.8681	−45.3524	3.78±0.25 (3)	306±10 (7)	stars	Tr
ESO 324-024	PGC047171	201.9042	−41.4806	3.78±0.09 (1)	514±18 (12)	HI	Sdm
NGC 5206	PGC047762	203.4292	−48.1511	3.21±0.01 (1)	583±6 (13)	stars	$S0^-$
NGC 5237	PGC048139	204.4083	−42.8475	3.33±0.02 (1)	361±4 (4)	HI	BCD
NGC 5253	PGC048334	204.9792	−31.6400	3.55±0.03 (3)	407±3 (4)	HI	Sdm
dw1341-43		205.4032	−43.8553	3.53±0.04 (10)	636±14 (7)	stars	dSph
KKs 57	PGC2815823	205.4079	−42.5797	3.84±0.47 (1)	511±17 (7)	stars	Sph
KK 211	PGC048515	205.5208	−45.2050	3.68±0.14 (1)	600±31 (14)	stars	Sph
dw1342-43		205.6837	−43.2548	2.90±0.14 (10)	510±8 (7)	stars	Tr
ESO 325-011	PGC048738	206.2500	−41.8589	3.40±0.05 (1)	544±1 (15)	HI	dIrr
KKs 58	PGC2815824	206.5031	−36.3289	3.36±0.10 (10)	477±5 (7)	stars	dSph
KK 221	PGC166179	207.1917	−46.9974	3.82±0.07 (1)	507±13 (14)	stars	dIrr
ESO 383-087	PGC049050	207.3250	−36.0614	3.19±0.03 (1)	326±2 (4)	HI	Sdm
ESO174-001/KKs 57	PGC048937	206.9920	−53.3476	3.68*	686±1 (15)	HI	dIrr

Notes. The references are: (1): Karachentsev et al. (2013), (2): Bouchard et al. (2007), (3): Tully et al. (2015), (4): Koribalski et al. (2004), (5): Banks et al. (1999), (6): Tully et al. (2008), (7): Müller et al. (2020), (8): Jerjen et al. (2000b), (9): Saviane & Jerjen (2007), (10): Müller et al. (2019), (11): Jerjen et al. (2000a), (12): Doyle et al. (2005), (13): Peterson & Caldwell (1993), (14): Puzia & Sharina (2008), and (15): Kirby et al. (2012).

Положения и лучевые скорости

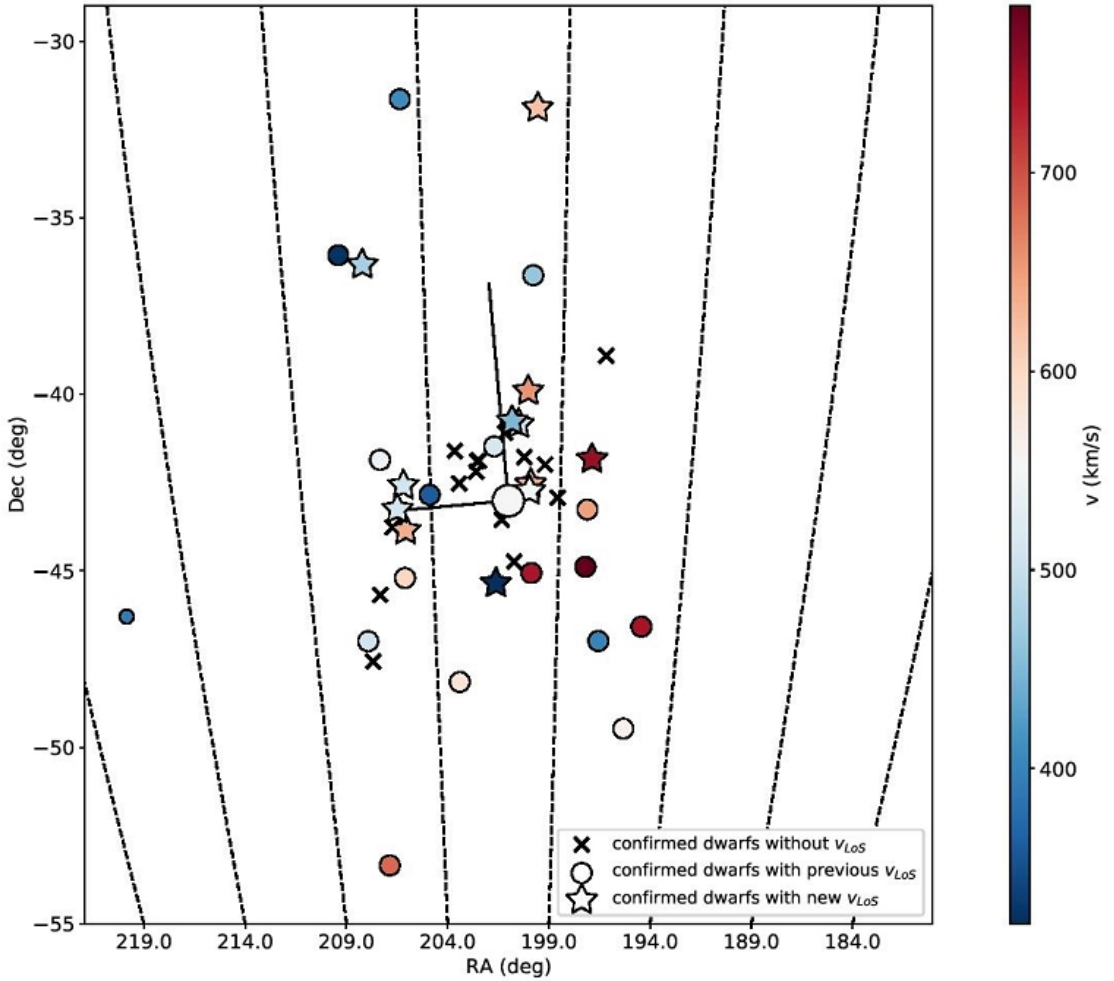

Fig. 1. The on-sky distribution of the Cen A satellite system within 800 kpc. The circles correspond to the dwarf galaxies studied in Müller et al. (2018a), the stars to the newly observed dwarfs (Müller et al. 2020). The colors indicate whether the galaxies are red-, or blue-shifted with respect to the systemic velocity of Cen A (shown with large open circle). The crosses are dwarf galaxies with known distances but without velocity

Таки-да, вращающийся диск!

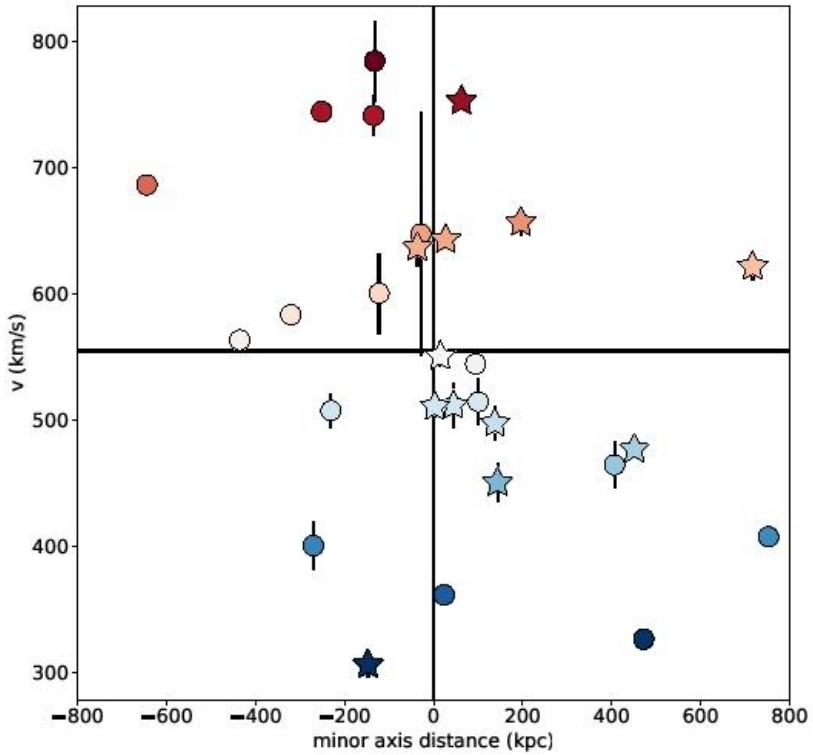

Fig. 2. Position-velocity diagram for the dwarf galaxy satellite system of Cen A. The x-axis represents the distance from the minor axis (i.e. along the major axis) derived from the satellite distribution. The filled circles show the dwarf galaxies used in Müller et al. (2018a), and the stars illustrate the new data. The uncertainties are always plotted, but often smaller than the dots. Approaching and receding galaxies with respect to the mean of the group are shown in blue and red, respectively, as in Fig 1.

Геометрические оси!

21 из 28 - в нужных квадрантах

Illustris-TNG100 дает только 0.2% таких систем!

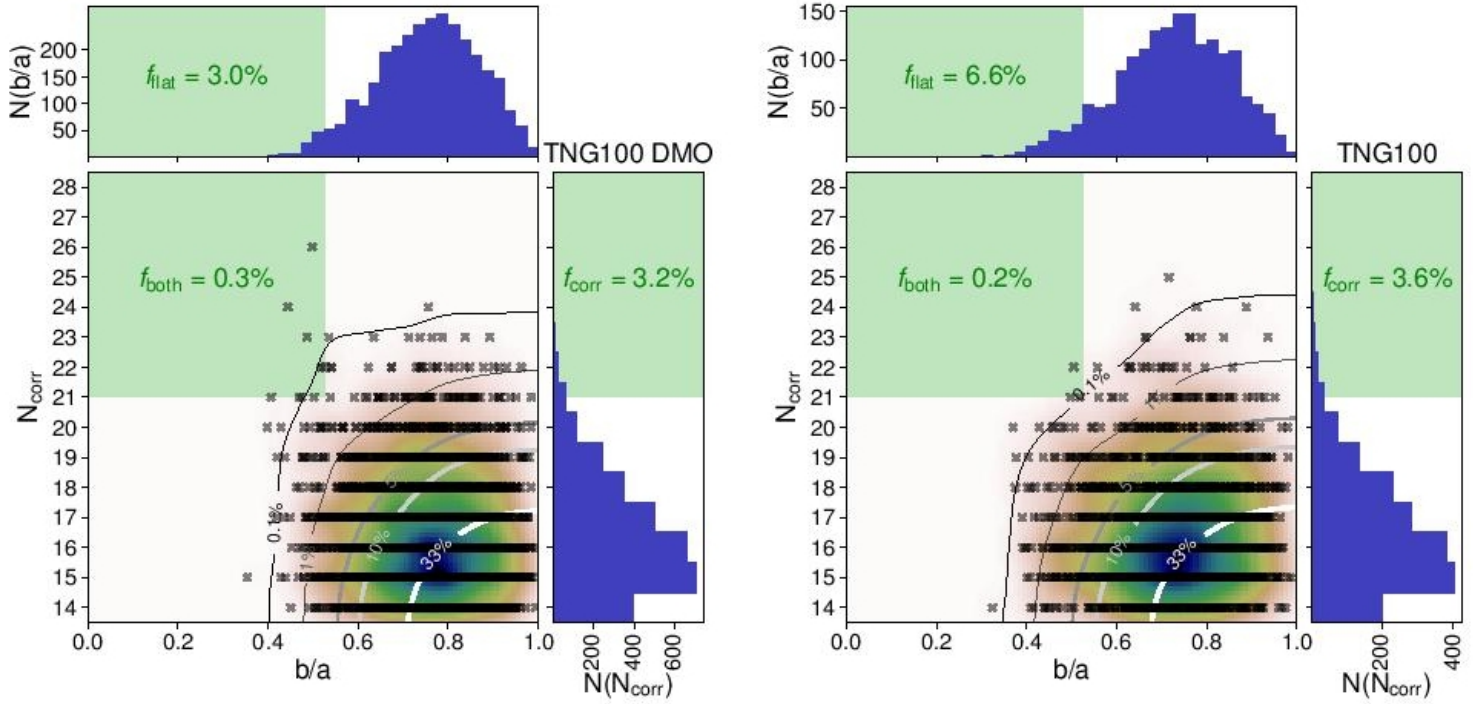

Fig. 3. Mock-observed satellite systems around Cen A analogs from the Illustris TNG-100 simulation, considering both its dark-matter-only run (left) and hydrodynamical run (right). The vertical axis plots the number of kinematically correlated satellites N_{corr}, with $N_{corr} = 21$ for the observed Cen A system. The horizontal axis plots the on-sky axis-ratio flattening b/a. The histograms show the number of realizations with a given axis ratio $N(b/a)$ and a given number of correlated velocities $N(N_{corr})$, respectively. The color maps indicate the density of simulated systems, while the contours indicate what fraction of simulated systems are more extreme than the parameter combination. The green shaded regions indicate parameter combinations that are as extreme or more as the observed Cen A system, while f_{flat}, f_{corr}, and f_{both} report the fraction of mock systems that are at least as flattened as the observed system, at least as kinematically correlated, or both simultaneously.

Вот эти 3 модельные системы – и они транзиентны (проекция)!

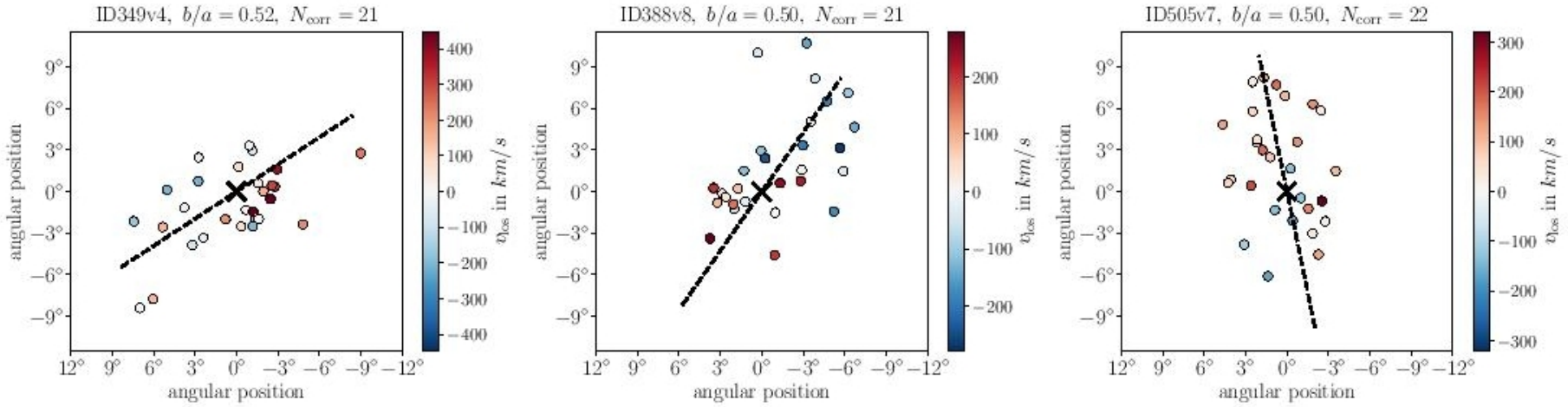

Fig. 4. Mock-observed on-sky satellite distributions of the three simulated systems that have satellite plane parameters as extreme as observed. The satellite galaxies (circles) are color coded by their line-of-sight velocity relative to the host (black cross). The dashed lines indicate the major axis of the projected distribution of satellites. The top labels give the minor-to-major axis flattening b/a of the on-sky distribution for the simulated systems, as well as the number of correlated velocities $N_{\rm corr}$.